Int. J. Heat Mass Transfer. Vol. 29, No. 10, pp. 1543–1552, 1986
Printed in Great Britain

0017-9310/86 $3.00 + 0.00
Pergamon Journals Ltd.

Natural convection flows in a vertical, open tube resulting from combined buoyancy effects of thermal and mass diffusion

C. J. CHANG,† T. F. LIN‡ and W. M. YAN
Department of Mechanical Engineering, National Chiao Tung University, Hsinchu, Taiwan, R.O.C.

(*Received* 31 *July* 1985 *and in final form* 7 *May* 1986)

Abstract—This study aims to investigate theoretically the role of latent heat transfer, in connection with the vaporization of a thin liquid film on a tube's inside surface, in natural convection flows driven by the simultaneous presence of combined buoyancy effects of thermal and mass diffusion. Results are specifically presented for an air–water system under various conditions. The effects of tube length and system temperatures on the momentum, heat and mass transfer in the flow are examined in great detail. The important role that the liquid film plays under the situations of buoyancy-aiding and opposing flows is clearly demonstrated.

INTRODUCTION

SITUATIONS often arise in which the combined buoyancy forces of thermal and mass diffusion—resulting from the simultaneous presence of differences in temperature and variations in concentration—have rather significant influences on heat transfer of flowing gas mixtures in engineering systems and the natural environment. Calm-day evaporation and vaporization of mist and fog are examples of such flow occurring in nature. Thermo-solutal or double-diffusive convection is a very common phenomenon in ocean flows. Even in human bodies the simultaneous diffusion of metabolic heat and perspiration control our body temperature especially on hot summer days. Distillation of a volatile component from a mixture with involatiles and cooling of a high temperature surface by coating it with certain types of evaporating material are just some prominent examples of such processes in which mass transfer operations are generally accompanied by the transfer of heat.

Steady natural convection flows induced by the buoyancy force of thermal diffusion in vertical, parallel plate channels [1, 2] and in vertical tubes [3–5] have been studied in detail. In contrast to forced convection, the magnitude and shape of the inlet velocity for natural convection flow in a channel are not known *a priori*. Uniform or parabolic inlet velocity profile was normally assumed in these studies. Transient laminar natural convection between heated, vertical plates including entrance effects was investigated by Kettleborough [6] and Nakamura *et al.* [7]. They found that for a small Grashof number a near-parabolic type of velocity distribution exists at the entry, while for a high Grashof number a velocity distribution with a minimum at the center of the entry exists at the steady-state. Recently, heat transfer in the buoyancy-induced flow—caused only by the temperature nonuniformity—in a vertical, internally finned duct was examined by Prakash and Liu [8].

The effects of mass diffusion on natural convection flows have been widely studied for flows over plates with different inclinations [9–16] and for flows over vertical cylinders [17]. Hason and Mujumdar [18] recently examined the flow along a vertical, circular cone and reported that the local Nusselt number and wall shear stress increase as the buoyancy force from species diffusion aids the thermal buoyancy force. The reverse is true when the two buoyancy forces act in opposite directions. This was also found by Chen and Yuh [17]. Recently, natural convection in a vertical plate channel within which the buoyancy force reverses its sign was studied by Lee *et al.* [19], where the effects of injection rate and wall temperature on flow characteristics were examined in great detail.

In the analyses mentioned above for the study of heat and mass transfer in natural convection flows, considerations were mainly placed on the external flow systems (except that of Lee *et al.* [19]). Thus, to a good approximation, the interfacial concentrations of the species are assumed to be constant. The analysis is then greatly simplified. For internal flow systems, it is no longer good enough to consider the interfacial concentrations to be constant because of the variation of pressure along the channel [20].

Recognizing the relatively little research on internal flow systems, the present authors [20] performed an analysis to study the nature of natural convection flows in a semi-infinite, vertical tube resulting from the combined buoyancy forces of thermal and mass diffusion, particularly for an air–water vapor mixture. In practical applications, channels of finite length are of great interest.

The work of ref. [20] is extended here to investigate the effects of the coupled thermal and mass diffusion

† Present address: Department of Mechanical Engineering, University of California, Berkeley, CA 94720, U.S.A.
‡ To whom correspondence should be addressed.

NOMENCLATURE

A	$[(c_{p1}-c_{p2})/c_p]\cdot(w_r-w_0)$
B	$\rho\cdot l^2\cdot v^2/(R^4\cdot p_w)$
C	p_0/p_w
c_p	specific heat
D	mass diffusivity
g	gravitational acceleration
Gr_M	Grashof number (mass transfer)
Gr_{Mr}	reference Grashof number (mass transfer)
Gr_T	Grashof number (heat transfer)
Gr_{Tr}	reference Grashof number (heat transfer)
h_{fg}	latent heat of vaporization
h_M	local mass transfer coefficient
k	thermal conductivity
l	tube length
l_r	reference tube length, 1 m
L	dimensionless tube length, $1/(Gr_{Tr}+Gr_{Mr})$
L_i	computed tube length during iteration i
M	molecular weight
Nu_l	local Nusselt number (latent heat)
Nu_s	local Nusselt number (sensible heat)
Nu_x	overall local Nusselt number
n_1	absolute mass flux of water vapor
p	pressure of the moist air in the tube
P	dimensionless motion pressure (pressure defect)
p_m	motion pressure (pressure defect), $p-p_0$
p_0	ambient pressure
Pr	Prandtl number, v/α
p_w	partial pressure of water vapor at interface
Q	total heat transfer rate
Q_0	total heat transfer rate without liquid water film
q''_x	interfacial energy flux flowing into air stream
r	radial coordinate
R	tube radius
Re	Reynolds number at inlet, $u_1(2R)/v$
S	parameter, equation (22)
Sc	Schmidt number, v/D
Sh_x	local Sherwood number
T	temperature
u	axial velocity
u_1, U_1	inlet velocities
U	dimensionless axial velocity
v	radial velocity
V	dimensionless radial velocity
V_w	dimensionless interfacial velocity of mixture
w_1	mass fraction of water vapor
W	dimensionless mass fraction of water vapor
w_r	saturated mass fraction of water vapor at T_w and p_0 at entry end
x	axial coordinate.

Greek symbols

α	thermal diffusivity
η	dimensionless radial coordinate
θ	dimensionless temperature, $(T-T_0)/(T_w-T_0)$
θ'	dimensionless temperature, $(T-T_w)/(T_0-T_w)$
ν	kinematic viscosity
ξ	dimensionless axial coordinate
ρ	density
ϕ	relative humidity of air at ambient condition.

Subscripts

1	of water vapor
2	of air
w	condition at interface
0	at ambient condition
r	at reference condition
b	bulk quantity
s	semi-infinite tube.

Superscript

*	at fully developed condition.

on the steady development of velocity, temperature and concentration fields in the natural convection flow of an air–water vapor mixture in a finite, vertical tube. Particular attention is paid to studying the extent of heat transfer enhancement through mass diffusion when the buoyancy forces are in the same direction and the reduction of heat transfer when they are in the opposite direction.

ANALYSIS

The system being investigated is an open-ended, vertical tube of finite length with a thin liquid water film on the inside surface of the tube (see Fig. 1). The tube wall is maintained at a uniform temperature T_w. The moist air in the ambient is drawn into the tube by the simultaneous action of combined buoyancy forces due to the differences in temperature and in concentration of water vapor between the liquid film and the ambient. Since the molecular weight of water vapor is smaller than that of air, the buoyancy force due to mass transfer acts upward. As a result, the flow induced by the buoyancy force of mass transfer is aided by the buoyancy force of heat transfer if $T_w > T_0$. While the flow is retarded if $T_w < T_0$.

As a preliminary attempt to study the mass diffusion

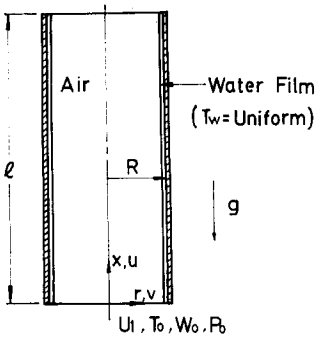

FIG. 1. Schematic diagram of the system.

effects, the liquid film on the tube's inside surface is assumed to be extremely thin so that it can be regarded as a boundary condition for heat and mass transfer—the film is stationary and at the same uniform temperature with the tube wall T_w. In reality the liquid film is finite in thickness. The film could be moving upwards or downwards, and the shape of the liquid–gas interface could be quite complex. As a result, the momentum, heat and mass transfer in the film should also be analyzed with the interfacial phenomena appropriately treated. This would, however, greatly complicate the analysis and make the theoretical work formidable. The influences of the finite liquid film on the heat transfer may not be properly assessed without the help from the experimental study which will be conducted shortly.

The formulation for the problem to be given in the following is rather brief with the complete details being available in the previous study [20]. By introducing the Boussinesq approximation (the concentration of water vapor in the mixture being very low and the temperature nonuniformity in the system being small), the steady natural convection flow of moist air in a vertical tube resulting from the combined buoyancy effects of thermal and mass diffusion can be described by the basic equations, in dimensionless form, as:

continuity equation

$$\frac{\partial(\eta U)}{\partial\xi}+\frac{\partial(\eta V)}{\partial\eta}=0 \tag{1}$$

axial-momentum equation

$$U\frac{\partial U}{\partial\xi}+V\frac{\partial U}{\partial\eta}=-\frac{\mathrm{d}P}{\mathrm{d}\xi}\pm\left(\frac{Gr_T\theta+Gr_M W}{Gr_{Tr}+Gr_{Mr}}\right)+\frac{1}{\eta}\frac{\partial}{\partial\eta}\left(\eta\frac{\partial U}{\partial\eta}\right) \tag{2}$$

energy equation

$$U\frac{\partial\theta}{\partial\xi}+V\frac{\partial\theta}{\partial\eta}=\frac{1}{Pr}\frac{1}{\eta}\frac{\partial}{\partial\eta}\left(\eta\frac{\partial\theta}{\partial\eta}\right)+\frac{A}{Sc}\frac{\partial\theta}{\partial\eta}\frac{\partial W}{\partial\eta} \tag{3}$$

species diffusion equation

$$U\frac{\partial W}{\partial\xi}+V\frac{\partial W}{\partial\eta}=\frac{1}{Sc}\frac{1}{\eta}\frac{\partial}{\partial\eta}\left(\eta\frac{\partial W}{\partial\eta}\right). \tag{4}$$

In nondimensionalizing the governing equations, the following dimensionless variables were introduced:

$$\begin{gathered}\xi=x/[l(Gr_{Tr}+Gr_{Mr})],\quad \eta=r/R\\ U=uR^2/[lv(Gr_{Tr}+Gr_{Mr})],\quad V=vR/v\\ \theta=(T-T_0)/(T_w-T_0),\quad W=(w_1-w_0)/(w_r-w_0)\\ P=p_m R^4/[\rho l^2 v^2(Gr_{Tr}+Gr_{Mr})^2].\end{gathered} \tag{5}$$

Here w_r is the saturated mass fraction of water vapor at T_w and p_0. Gr_{Tr} and Gr_{Mr} are respectively the Grashof numbers for heat transfer and mass transfer at the reference condition which is chosen to be $T_0 = 20°C$, $T_w = 40°C$, $p_0 = 1$ atm, $\phi = 50\%$ and $l = 1.0$ m. The use of Gr_{Tr} and Gr_{Mr} leads to a physically more meaningful comparison among various cases studied [20]. This will become clear later. The Grashof numbers are defined as

$$Gr_T=g(T_w-T_0)R^4/(lv^2T_0) \tag{6}$$

$$Gr_M=g(M_2/M_1-1)(w_r-w_0)R^4/(lv^2). \tag{7}$$

In writing the basic equations the boundary-layer approximation has been made and the presence of the tube exit on the flow and thermal fields is presumed to be insignificant, which is a good approximation when $l \gg R$ [21, 22]. The last term on the RHS of equation (3) signifies the energy transport through the interdiffusion of the species, air and water vapor. The second term on the RHS of equation (2) represents the momentum transfer caused by the combined buoyancy forces. It is positive when the flow moves upwards, and the x-coordinate is chosen such that $x = 0$ is at the bottom end of the tube and increases upwards. For the flow moving downwards it is negative, and $x = 0$ is placed at the top end of the tube and increases downwards. The adoption of such different coordinate systems facilitates the analysis of natural convection flow with aiding or opposing buoyancy forces.

Making use of the equation of state for the ideal gas mixture and assuming low water vapor concentration, the density variation in the moist air can be approximated by

$$\frac{\rho_0-\rho}{\rho}=\frac{1}{T_0}(T-T_0)+(M_2/M_1-1)\cdot(w_1-w_0). \tag{8}$$

Assuming that the air–water interface is semi-permeable—that is, the solubility of air in water is negligibly small and air is stationary at the interface—the velocity of water vapor at the interface can be obtained as [23]

$$v_w=-\frac{D}{1-w_w}\frac{\partial w_1}{\partial r}\bigg|_{r=R}. \tag{9}$$

According to Dalton's law and the equation of state for ideal gas mixture, the interfacial mass fraction of water vapor can be calculated by

$$w_w=\frac{p_w M_1}{p_w M_1+(p-P_w)M_2} \tag{10}$$

where p_w is the partial pressure of water vapor at the interface. Since vaporization takes place at the interface, p_w is the saturated vapor pressure of water at the interfacial temperature. In other words, thermodynamic equilibrium is assumed to exist at the interface. It is worth noting from equation (10) that w_w is dependent on the mixture pressure p, and thus it varies with x. This prevents us from taking w_w as a reference value in the nondimensionalization process. Equations (1)–(4) are subject to the following boundary conditions

$$\begin{gathered}\xi = 0, \quad U = U_1, \quad \theta = 0, \quad W = 0, \quad P = 0 \\ \eta = 0, \quad \partial U/\partial\eta = 0, \quad \partial\theta/\partial\eta = 0, \quad \partial W/\partial\eta = 0 \\ \eta = 1, \quad U = 0, \quad V = V_w, \quad \theta = 1 \\ W = (w_w - w_0)/(w_r - w_0) \\ \xi = 1/(Gr_{Tr} + Gr_{Mr}), \quad P = 0.\end{gathered} \tag{11}$$

Here

$$V_w = -\frac{w_r - w_0}{1 - w_w}\frac{1}{Sc}\left.\frac{\partial W}{\partial\eta}\right|_{\eta=1} \tag{12}$$

$$w_w = \{1 + [B(Gr_{Tr} + Gr_{Mr})^2 p + C - 1] \cdot M_2/M_1\}^{-1}. \tag{13}$$

It should be noted that both the magnitude and shape of the inlet velocity U_1 are not known before the complete solution for the governing equations, including the entrance and end effects, is obtained [6, 7]. In the previous investigation [20], it was shown that the magnitude of U_1 can be determined from the solution processes, and the shape of U_1 has little effect on the heat and mass transfer in the flow. Thus, in the present study U_1 is assumed to be uniform, and its magnitude will be found by the iterative procedures in the numerical solution.

One constraint to be satisfied in the analysis of a steady channel flow is the overall mass balance at every axial location

$$\int_0^1 U \cdot \eta \, d\eta = \frac{U_1}{2} - \int_0^\xi V_w \, d\xi. \tag{14}$$

The above equation is used in the solution process to check whether the pressure gradient in the flow is correctly guessed.

As is mentioned earlier, the magnitude of U_1 is not known before the solution is completed. However, knowing the inlet velocity U_{1s} for the case of a long tube in which the flow can reach fully developed conditions is of much help to our initial guess of U_1 for the case of a finite tube. The magnitude of U_{1s} can be obtained [20] through the use of the fully developed conditions and the overall conservation of mass, equation (14). The result for U_{1s} is

$$U_{1s} = \frac{1}{8}\left(Gr_T + Gr_M \cdot \frac{w^* - w_0}{w_r - w_0}\right)\Big/(Gr_{Tr} + Gr_{Mr}) + 2\int_0^{\xi^*} V_w \, d\xi. \tag{15}$$

Since V_w, w^* and ξ^* are unknown parameters before the complete solution is available, it is desirable to make such approximations: $V_w = 0$ and $w^* = w_r$. The approximate value of U_{1s} is then obtained as

$$U_{1s} = \tfrac{1}{8}(Gr_T + Gr_M)/(Gr_{Tr} + Gr_{Mr}). \tag{16}$$

Energy transport between the tube wall and the moist air in the presence of mass transfer depends on two related factors: the fluid temperature gradient at the wall and the rate of mass transfer. The connection of energy transfer with these factors is obtained by means of an interfacial energy balance [23, 24]

$$q_x'' = k \cdot \left.\frac{\partial T}{\partial r}\right|_{r=R} + \frac{\rho D h_{fg}}{1 - w_w}\left.\frac{\partial w_1}{\partial r}\right|_{r=R}. \tag{17}$$

A local Nusselt number is defined as

$$Nu_x = \frac{2R}{k} \cdot \frac{q_x''}{T_w - T_b}. \tag{18}$$

This leads to

$$Nu_x = Nu_s + Nu_l \tag{19}$$

where

$$Nu_s = \frac{2}{1 - \theta_b} \cdot \left.\frac{\partial\theta}{\partial\eta}\right|_{\eta=1} \tag{20}$$

$$Nu_l = \frac{2S}{(1 - \theta_b)(1 - w_w)} \cdot \left.\frac{\partial W}{\partial\eta}\right|_{\eta=1}. \tag{21}$$

Here S signifies the relative importance of energy transport through species diffusion to that through thermal diffusion

$$S = \rho D h_{fg} \cdot (w_r - w_0)/k \cdot (T_w - T_0). \tag{22}$$

The mass flux of water vapor flowing into the air stream at the interface is given as

$$n_1 = \frac{\rho D}{1 - w_w} \cdot \left.\frac{\partial w_1}{\partial r}\right|_{r=R}. \tag{23}$$

For slow mass transfer rate at the interface, which happens to be the case in the present study, a mass transfer coefficient h_M can be defined as

$$n_1(1 - w_w) = \rho h_M (w_w - w_b). \tag{24}$$

The local Sherwood number then becomes

$$Sh_x = \frac{h_M(2R)}{D} = 2\left(\frac{w_r - w_0}{w_w - w_b}\right) \cdot \left.\frac{\partial W}{\partial\eta}\right|_{\eta=1}. \tag{25}$$

SOLUTION METHOD

Because the flow under consideration is a boundary-layer type, the solution for equations (1)–(4) can be marched in the downstream direction. A fully implicit numerical scheme in which the axial convection is approximated by the upstream difference and the radial convection and diffusion terms by the central difference is employed to transform the governing equations into finite-difference equations. Each system of the finite-

difference equations forms a tridiagonal matrix which can be efficiently solved by the Thomas Algorithm [25]. For a given condition, a brief outline of the solution procedures is described as follows:

(1) Guess an inlet velocity U_1 (smaller than U_{1s}).
(2) For any axial location, guess $(dp/d\xi)$ and solve the finite-difference forms of equations (2)–(4) for U, θ and W.
(3) Integrate the continuity equation numerically to find V

$$V = -\frac{1}{\eta}\frac{\partial}{\partial \xi}\int_0^{\eta} U \cdot \eta \, d\eta. \tag{26}$$

(4) Check the satisfaction of the overall conservation of mass, equation (14). If yes, continue the above procedures for the next axial location. If not, guess a new $(dp/d\xi)$ and repeat procedures (2)–(4) for the current location.
(5) Procedures (2)–(4) are successively applied to every axial location from the tube entrance to the downstream region where the motion pressure first becomes positive.
(6) Employ linear interpolation to evaluate the dimensionless tube length L_i, a distance between the tube entrance and the downstream location where $P = 0$.
(7) Check if $|L_i - L| < \varepsilon$, where ε is chosen to be 0.001 in computation. If yes, the solution is completed. If not, guess a new U_1 and repeat procedures (2)–(7) until L_i is very close to L.

The above procedures differ slightly from those adopted for the analysis of natural convection in vertical channels induced by the single buoyancy force of heat transfer [2, 4]. For the flow driven by the combined buoyancy forces of heat and mass transfer, the tube length determined by the scheme used in refs. [2, 4] may not correspond to a real physical situation for a given gas mixture. Thus the present scheme is adopted.

As is already mentioned, the flow in the tube can move upwards or downwards, depending upon the value for $(Gr_T\theta + Gr_M W)$ being positive or negative. Because the air–water vapor mixture is considered ($Pr = 0.7$, $Sc = 0.6$), the concentration boundary layer develops almost at the same rate as the temperature boundary layer does. Consequently, the direction of the flow in the tube can be approximately judged as follows:

upward flow when $(Gr_T + Gr_M) > 0$

downward flow when $(Gr_T + Gr_M) < 0$.

This criterion is very useful in our numerical computations.

In the solution of finite-difference equations by the Thomas Algorithm, a successive under-relaxation numerical scheme is used. It is found that the computer time can be saved by about 30% with a relaxation factor of 0.8 which is consistent with the findings in ref. [25].

A uniform grid is placed in the radial direction, which is believed to be appropriate in the consumption of laminar flows, while in the axial direction a nonuniform grid is employed to account for the drastic variations of U, θ and W in the near-entrance region. A 41×30 grid is used in the actual computations. For all cases studied it took less than 120 s to obtain the solution with a CDC (Control Data Corporation) Cyber 170/720 computer system.

RESULTS AND DISCUSSION

To verify the numerical scheme outlined above for the problem under consideration, the results for the limiting case of natural convection flows in a vertical tube induced by the buoyancy force of thermal diffusion alone were first obtained. Excellent agreement between the present prediction and that of Davis and Perona [4] was found.

In this study the calculations are specifically performed for moist air flowing in the tube, a situation widely found in engineering systems. Other mixtures can be analyzed in the same way. It should be recognized herein that not all the values for the nondimensional groups appearing in the analysis, i.e. Pr, Sc, Gr_T, Gr_M, etc., can be arbitrarily assigned. In fact, they are interdependent for a given mixture under certain specified conditions. To be physically meaningful T_0, T_w, P_0, ϕ and l are chosen as the independent parameters.

In order to investigate the effect of wall and ambient conditions on the development of velocity, temperature and mass-fraction profiles as well as on the characteristics of heat and mass transfer, the cases given in Table 1 are selected for the computations. Here the reference case mentioned previously is indicated in the last row of Table 1. This is used to define Gr_{Tr} and Gr_{Mr}, the Grashof numbers at reference condition. Though defying reality, the choice of 0% relative humidity is to study the characteristics of flow and heat transfer with the buoyancy forces in the opposite direction when air in the ambient is relatively dry. All the above cases are based on a 2-cm-diameter, finite, vertical tube.

Shown in Fig. 2 are the development of the axial velocity in the tube under various conditions. It is clearly seen that the mass flowrate of the moist air in the tube keeps increasing as the air moves downstream owing to the evaporation of water vapor into the air stream from the liquid film. A rise in T_w [Fig. 2(b)] results in higher axial velocity U, in conformity with the fact that a greater amount of water vapor evaporates into the flow for a higher T_w and a larger buoyancy force through thermal diffusion. When the tube is short [Fig. 2(c)], the velocity profiles near the tube exit become distorted. Maximum velocity is off the centerline. In reality, a shorter tube gives higher

Table 1

Case	T_0	T_w	p_0	ϕ	l	Gr_T	Gr_M	S
I	20	40	1	50	0.4	64	23	5.40
II	20	60	1	50	0.4	112	62	8.18
III	40	20	1	0	0.4	−64	9	−2.05
IV	60	20	1	0	0.4	−112	8	−1.02
V	20	40	1	50	0.12	214	75	5.40
VI	20	40	2	50	0.4	64	11	1.34
Ref.	20	40	1	50	1.0	26	9	5.40

Units for parameters: T in °C, p_0 in atm, ϕ in %, l in m.

Gr_T and Gr_M. Thus the buoyancy effect is more pronounced. Illustrated in Fig. 2(d) is the development of an opposing flow in which the buoyancy force resulting from the thermal diffusion ($Gr_T = -64$) overcomes the buoyancy force from the mass diffusion ($Gr_M = 9$). The combined effect is that the ambient air is driven into the tube from the top end and moves in the downward direction. Notice that the flow moves more slowly because of smaller $(Gr_T + Gr_M)$. An increase in p_0 (case VI) leads to a smaller axial velocity, in agreement with a smaller driving force due to mass transfer Gr_M.

The development of temperature profiles are plotted in Fig. 3. Comparison of corresponding curves in Figs. 3(a) and (b) at the same x/l indicates that a shorter tube develops a somewhat steeper temperature gradient at the tube wall. This implies that a shorter tube can transport sensible energy more effectively on the basis of the same unit surface area, which is simply caused by the more pronounced entrance effect for the shorter tube. At higher ambient pressure p_0 [Fig. 3(c)] slightly faster development in θ is observed. The opposing flow shown in Fig. 3(d) has different shapes of temperature profiles, where θ' $(= 1-\theta)$ is plotted. The switchover from θ to θ' is consistent with the physical situation that the flow entering the tube is at a higher temperature. The sensible heat transfer is, therefore, from the moist air to the tube wall.

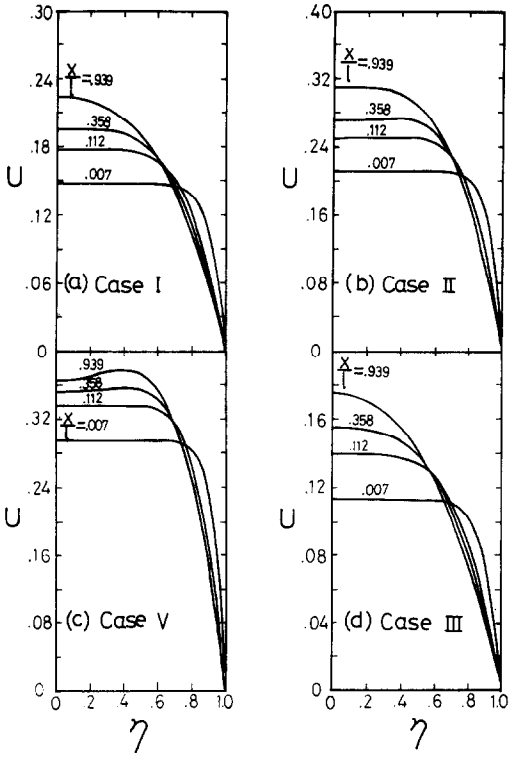

FIG. 2. Development of dimensionless axial velocity profiles: (a) $T_0 = 20°C$, $T_w = 40°C$, $p_0 = 1$ atm, $\phi = 50\%$, $l = 0.4$ m; (b) $T_w = 60°C$; (c) $l = 0.12$ m; (d) $T_0 = 40°C$, $T_w = 20°C$, $\phi = 0\%$.

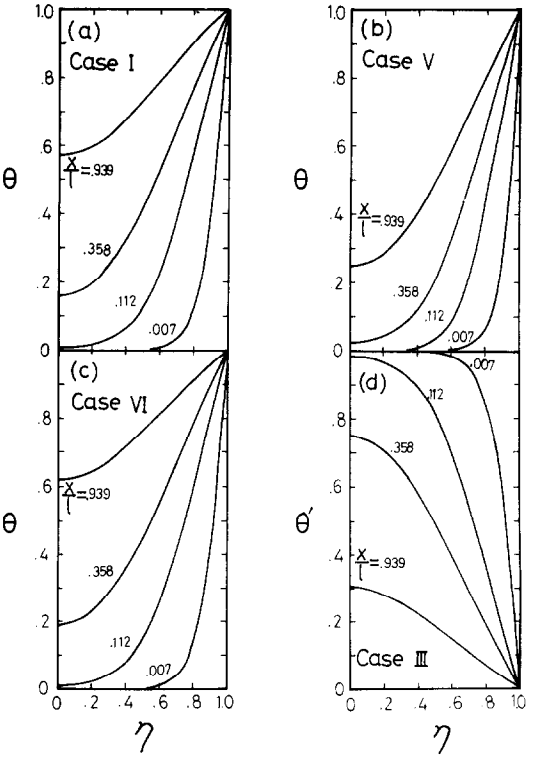

FIG. 3. Development of dimensionless temperature profiles: (a) $T_0 = 20°C$, $T_w = 40°C$, $p_0 = 1$ atm, $\phi = 50\%$, $l = 0.4$ m; (b) $l = 0.12$ m; (c) $p_0 = 2$ atm; (d) $T_0 = 40°C$, $T_w = 20°C$, $\phi = 0\%$.

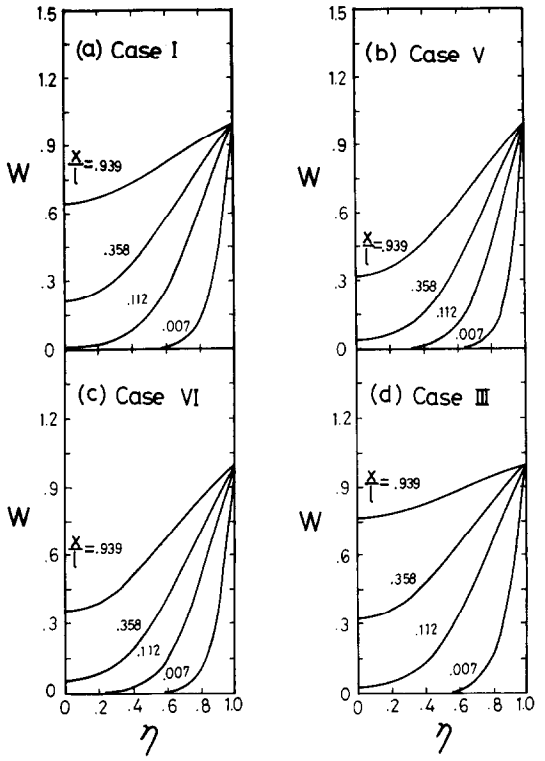

FIG. 4. Development of dimensionless mass-fraction profiles: (a) $T_0 = 20°C$, $T_w = 40°C$, $p_0 = 1$ atm, $\phi = 50\%$, $l = 0.4$ m; (b) $l = 0.12$ m; (c) $p_0 = 2$ atm; (d) $T_0 = 40°C$, $T_w = 20°C$, $\phi = 0\%$.

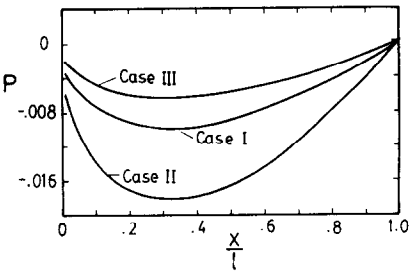

FIG. 5. Dimensionless motion pressure distributions along the tube. Case I: $T_0 = 20°C$, $T_w = 40°C$, $p_0 = 1$ atm, $\phi = 50\%$, $l = 0.4$ m; Case II: $T_w = 60°C$; Case III: $T_0 = 40°C$, $T_w = 20°C$, $\phi = 0\%$.

In line with the evaporation of water vapor into the air stream, the mass fraction of water vapor shown in Fig. 4 increases gradually as the air moves in the tube. A higher mass-fraction of water vapor is found at the exit of the longer tube by comparing Figs. 4(a) and (b). This is a direct consequence of a larger amount of water vapor entering the air stream from the vaporization of the liquid film. If the ambient pressure p_0 goes higher [Fig. 4(c)], W accordingly goes lower. This can be justified by realizing the fact that the lower water vapor mass fraction exists at the interface for higher p_0, equation (10). Opposing flow [Fig. 4(d)] shows the same trend as aiding flow.

It is interesting to note that the pressure defect in the flow given in Fig. 5 increases with x up to about $x = 0.3l$, but beyond that point it decreases to meet the boundary condition: $P = 0$ at $x = l$. In every case studied, the trend for the development of the pressure defect is the same, and the largest pressure defect always appears around $x/l = 0.3$. Similar results were noted by Davis and Perona [4] when the mass diffusion effect is absent. The maximum pressure defect appears at $x/l = 0.33$ for a tube with a uniform wall temperature in their analysis. In addition, it is observed qualitatively that the higher the combined driving forces ($Gr_T + Gr_M$), the larger the pressure defect. One point worth mentioning is that the pressure defect in the flow resulting from the combined buoyancy forces is small enough to keep w_w very close to w_r [20]. This gives $W = 1$ at the interface as is evident in Fig. 4.

To study the relative contributions of heat transfer through sensible and latent heat exchanges in the flow, three kinds of Nusselt number are presented in Fig. 6. Regarding Nu_s-curves, only slight differences exist among various cases. While in Nu_l-curves, the deviations among cases are rather substantial. The negative values for Nu_l in Figs. 6(b) and (c) result directly from the definition of S, equation (22), which is negative when opposing flow is concerned. In other words, negative Nu_l simply indicates that the direction of latent heat exchange is opposed to that of sensible heat exchange. This can be understood by recognizing that Nu_s defined in equation (20) is always positive,

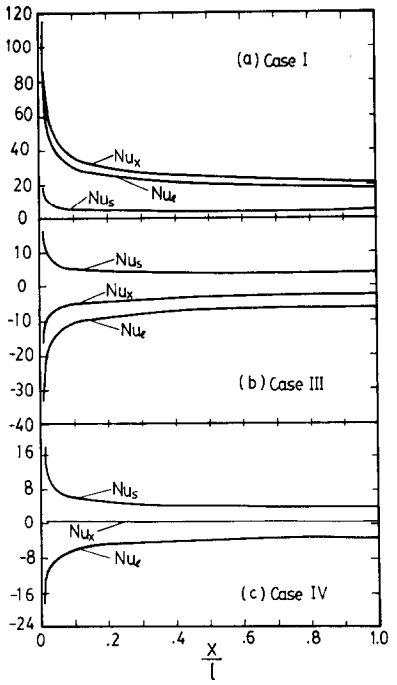

FIG. 6. Local Nusselt number distributions along the tube: (a) $T_0 = 20°C$, $T_w = 40°C$, $p_0 = 1$ atm, $\phi = 50\%$, $l = 0.4$ m; (b) $T_0 = 40°C$, $T_w = 20°C$, $\phi = 0\%$, (c) $T_0 = 60°C$, $T_w = 20°C$, $\phi = 0\%$.

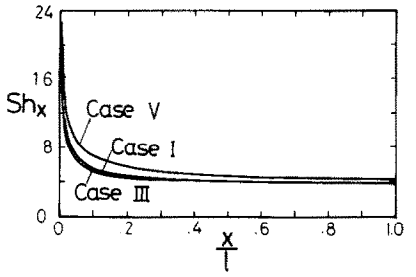

FIG. 7. Local Sherwood number distributions along the tube. Case I: $T_0 = 20°C$, $T_w = 40°C$, $p_0 = 1$ atm, $\phi = 50\%$, $l = 0.4$ m; Case III: $T_0 = 40°C$, $T_w = 20°C$, $\phi = 0\%$; Case V: $l = 0.12$ m.

irrespective of the heat transfer direction. In aiding flow [Fig. 6(a)], latent heat transport dominates over the sensible heat transfer. In opposing flow [Fig. 6(b)], it is interesting to find that the overall Nusselt number Nu_x is negative. Physically speaking, the liquid film not only serves as a heat barrier to protect the tube wall but also transports energy from the tube wall to the air stream through vaporization of the liquid film. The superiority of film cooling is thus justified. When the ambient temperature T_0 goes higher [Fig. 6(c)], the latent heat transport is overwhelmed by the sensible heat transport, which leads to a positive Nusselt number Nu_x.

The variation of local Sherwood number Sh_x, shown in Fig. 7, resembles that of Nu_s because Pr ($= 0.7$) is close to Sc ($= 0.6$). Sh_x is higher for the shorter tube, indicating that mass transfer (vaporization of liquid film) is more effective for a short tube. Again this is due to the larger entrance effect. On the other hand, it is lower for the opposing flow because of the smaller Gr_M. This deviation, however, reduces in the downstream direction. In effect, Sh_x approaches a constant value of 3.66 in the fully developed region of a semi-infinite tube as was discussed in separate studies [20, 26].

How much air is driven into the vertical tube under the action of the combined buoyancy forces is an important characteristic of the problem studied. This is investigated in Fig. 8, where the Reynolds number of the flow based on the inlet velocity is plotted. For a given curve the tube length is varied with other parameters (T_0, T_w, p_0, ϕ) fixed. The reference tube length l_r is chosen to be 1 m. The higher flowrate at the tube inlet is found to be associated with the longer tube. This can be readily explained by expressing Re in terms of U_1 and l through the use of equation (5)

$$Re = u_1 \cdot (2R)/\nu = 2U_1 l(Gr_{T_r} + Gr_{M_r})/R. \quad (27)$$

When the tube becomes longer, the dimensionless axial velocity at inlet U_1 is somewhat reduced but not in direct proportion to the increase in l, as is clearly seen by examining Figs. 2(a) and (c). The net effect is then an increase in Re. In a short tube the increase in Re with l is rather significant. While for a long tube the increase is gradual. For the asymptotic case of a semi-infinite tube Re remains unchanged [26].

The effect of system temperatures on the Reynolds number is also shown in Fig. 8, where case I″ represents the same situation as case I except that there is no liquid film on the inside surface of the tube. The existence of the liquid film (case I) introduces an additional buoyancy force through mass diffusion in conjunction with the liquid film vaporization. An increase in the Reynolds number by about 20% is observed. A rise in T_w (case II) also causes larger buoyancy forces, both thermal and mass diffusion, and hence the higher Reynolds number. Regarding the downward flow for case III, it is seen that the Reynolds number is the smallest in four cases. This is justified by the fact that the combined buoyancy forces due to heat and mass transfer are opposed to each other.

To illustrate the effectiveness of latent heat transfer through mass diffusion, the total heat transfer rate Q from the tube to the moist air with the presence of the liquid film on the tube's inside surface is compared with the result obtained for the situation in which the liquid film is absent. The results for Q/Q_0 are given in Fig. 9, where Q_0 represents the total heat transfer rate for case I″. Q/Q_0 is about 7 for case I, while the increase in Re is only around 20%. Thus the latent heat transfer is predominant over the sensible heat transfer. The tremendous capability of energy transport through mass diffusion is clearly demonstrated by noting that Q/Q_0 can be as large as 36 when T_w is raised to 60°C. If

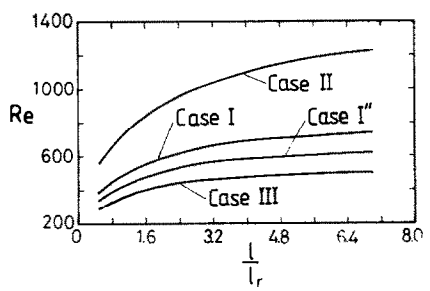

FIG. 8. Effect of tube length on the Reynolds number at the tube inlet. Case I: $T_0 = 20°C$, $T_w = 40°C$, $p_0 = 1$ atm, $\phi = 50\%$; Case II: $T_w = 60°C$; Case III: $T_0 = 40°C$, $T_w = 20°C$, $\phi = 0\%$; Case I″: without mass diffusion.

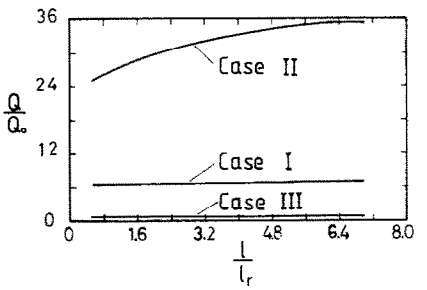

FIG. 9. Effect of system temperatures on the total heat transfer rate. Case I: $T_0 = 20°C$, $T_w = 40°C$, $p_0 = 1$ atm, $\phi = 50\%$; Case II: $T_w = 60°C$; Case III: $T_0 = 40°C$, $T_w = 20°C$, $\phi = 0\%$.

the liquid film is nonexistent, the increase is only about four times. For the case of downward flow (case III) where the buoyancy forces are in opposite direction, Q/Q_0 is only 0.67. This indicates that the tube wall is protected from the hot air.

CONCLUDING REMARKS

The nature of natural convection flows in a finite, vertical tube resulting from the combined buoyancy effects of thermal and mass diffusion has been studied, particularly for an air–water system. The effects of tube length as well as system temperatures and pressures on the heat and mass transfer in the flow are examined in great detail. The important role that the liquid water film plays is thoroughly investigated and clearly emphasized. What follows is a brief summary of the major results:

(1) Heat transfer in the flow is dominated by the transport of latent heat in association with the vaporization of the liquid film. For buoyancy-aiding flows vaporization greatly strengthens the cooling effect. While it serves as a heat barrier to protect the tube wall when the buoyancy forces are in opposite directions.
(2) A shorter tube gives steeper temperature and mass-fraction profiles, which in turn results in higher Nu_s and Sh_x.
(3) A rise in p_0 leads to a decrease in the mass fraction of water vapor and mass transfer Grashof number Gr_M. Therefore it reduces the effect of mass diffusion.
(4) The influences of the latent heat transport on the characteristics of heat transfer in the flow depend largely on the magnitude of the temperature difference $(T_w - T_0)$ and the directions of the buoyancy forces.

It is recognized herein that the results presented above are based on a number of assumptions made in the study. To test the validity of the assumptions, further research must be pursued. In short, we endeavor to extend the current research to cover the following aspects:

(i) A complete analysis to include the flow and thermal fields in the regions surrounding the tube ends.
(ii) The influence of a finite thickness liquid film in which the temperature is no longer uniform and the fluid in the film is flowing.
(iii) Conducting an experimental study to measure the quantities of interest—the velocity, temperature and concentration fields as well as the Nusselt numbers and heat transfer rates.

Additionally, it is realized that when the system operates at high temperatures, the use of the Boussinesq approximation (constant thermophysical properties except for density in the buoyancy term and linearization of buoyancy force variations with temperature and concentration) is simply inappropriate. This becomes a serious problem especially for an air–water system, inasmuch as water vapor saturated in air could be in significant amount when the mixture is at high temperature.

Acknowledgement—The authors wish to acknowledge the financial support of this work by National Science Council of Taiwan, R.O.C.

REFERENCES

1. J. R. Bodoia and J. F. Osterle, The development of free convection between heated vertical plates, *J. Heat Transfer* **84**, 40–44 (1962).
2. W. Aung, L. S. Fletcher and V. Sernas, Developing laminar free convection between vertical flat plates with asymmetric heating, *Int. J. Heat Mass Transfer* **15**, 2293–2308 (1972).
3. E. M. Rosen and T. J. Hanratty, Use of boundary-layer theory to predict the effect of heat transfer on the laminar-flow field in a vertical tube with a constant-temperature wall, *A.I.Ch.E. Jl* 7, 112–123 (1961).
4. L. P. Davis and J. J. Perona, Development of free convection flow of a gas in a heated vertical open tube, *Int. J. Heat Mass Transfer* **14**, 889–903 (1971).
5. M. Kageyama and R. Izumi, Natural heat convection in a vertical circular tube, *Bull. J.S.M.E.* **13**, No. 57, 382–394 (1970).
6. C. F. Kettleborough, Transient laminar free convection between heated vertical plates including entrance effects, *Int. J. Heat Mass Transfer* **15**, 883–896 (1972).
7. H. Nakamura, Y. Asako and T. Naitou, Heat transfer by free convection between two parallel flat plates, *Numer. Heat Transfer* **5**, 95–106 (1982).
8. C. Prakash and Y. D. Liu, Buoyancy induced flow in a vertical internally finned circular duct, *J. Heat Transfer* **107**, 118–123 (1985).
9. B. Gebhart and L. Pera, The nature of vertical natural convection flows resulting from the combined buoyancy effects of thermal and mass diffusion, *Int. J. Heat Mass Transfer* **14**, 2025–2050 (1971).
10. T. S. Chen and C. F. Yuh, Combined heat and mass transfer in natural convection on inclined surfaces, *Numer. Heat Transfer* **2**, 233–250 (1979).
11. W. G. Mathers, A. J. Madden, Jr. and E. L. Piret, Simultaneous heat and mass transfer in free convection, *I & EC Fund.* **49**, 961–968 (1957).
12. D. A. Saville and S. W. Churchill, Simultaneous heat and mass transfer in free convection boundary layers, *A.I.Ch.E. Jl* **16**, 268–273 (1970).
13. E. V. Somers, Theoretical considerations of combined thermal and mass transfer from a vertical flat plate, *J. appl. Mech.* **23**, 295–301 (1956).
14. W. N. Gill, E. D. Casal and D. W. Zeh, Binary diffusion and heat transfer in laminar free convection boundary layers on a vertical plate, *Int. J. Heat Mass Transfer* **8**, 1135–1151 (1965).
15. F. A. Bottemanne, Theoretical solution of simultaneous heat and mass transfer by free convection about a vertical flat plate, *Appl. Sci. Res.* **25**, 137–149 (1971).
16. V. M. Soundalgekar and P. Ganesan, Finite-difference analysis of transient free convection with mass transfer on an isothermal vertical flat plate, *Int. J. Engng Sci.* **19**, 757–770 (1981).
17. T. S. Chen and C. F. Yuh, Combined heat and mass transfer in natural convection along a vertical cylinder, *Int. J. Heat Mass Transfer* **23**, 451–461 (1979).

18. M. Hason and A. S. Mujumdar, Coupled heat and mass transfer in natural convection under flux condition along a vertical cone, *Int. Commun. Heat Mass Transfer* **11**, 157–172 (1984).
19. T. S. Lee, P. G. Parikh, A. Acrivos and D. Bershader, Natural convection in a vertical channel with opposing buoyancy forces, *Int. J. Heat Mass Transfer* **25**, 499–511 (1982).
20. T. F. Lin and C. J. Chang, Combined heat and mass transfer in natural convection flows in a vertical tube, 85-HT-26, 23rd National Heat Transfer Conference, Denver, CO (1985).
21. R. Yamaguchi and K. Takahashi, Flow pattern near the outlet of a straight long circular tube (1st report, experimental study of velocity profile), *Bull. J.S.M.E.* **23**, No. 185, 1798–1805 (1980).
22. R. Yamaguchi and K. Takahashi, Flow pattern near the outlet of a straight long circular tube (2nd report, theoretical calculation), *Bull. J.S.M.E.* **23**, No. 185, 1806–1813 (1980).
23. E. R. G. Eckert and R. M. Drake, Jr., *Analysis of Heat and Mass Transfer*, Chaps 20 and 22. McGraw-Hill, New York (1972).
24. J. L. Manganaro and O. T. Hanna, Simultaneous energy and mass transfer in the laminar boundary layer with large mass transfer rates toward the surface, *A.I.Ch.E. Jl* **16**, 204–211 (1970).
25. S. V. Patankar, *Numerical Heat Transfer and Fluid Flow*, Chap. 6. Hemisphere/McGraw-Hill, New York (1980).
26. T. F. Lin and C. J. Chang, Analysis of combined buoyancy effects of thermal and mass diffusion on laminar forced convection heat transfer in a vertical tube, HTD-Vol. 53, pp. 71–78, ASME Winter Annual Meeting, Miami, FL (1985).

CONVECTION NATURELLE, DANS UN TUBE VERTICAL OUVERT, SOUS L'EFFET COMBINE DE FORCES THERMIQUES ET MASSIQUES D'ARCHIMEDE

Résumé—On étudie théoriquement le rôle du transfert de chaleur latente en connection avec la vaporisation d'un film mince liquide sur la surface intérieure d'un tube, en convection naturelle conduite par les effets combinés de forces d'Archimède dues à la diffusion de la chaleur et de la masse. Des résultats sont présentés pour un système air–eau sous des conditions différentes. On examine en détail les effets de la longueur du tube et des températures sur le transfert de quantité de mouvement, de chaleur et de masse dans l'écoulement. Il est démontré clairement le rôle important que joue le film liquide dans les cas des écoulements aidés ou contrariés par les forces de gravité.

NATÜRLICHE KONVEKTIONSSTRÖMUNGEN IN EINEM SENKRECHTEN OFFENEN ROHR

Zusammenfassung—Ziel der Arbeit ist die theoretische Untersuchung der Übertragung von latenter Wärme, wie sie bei der Verdampfung eines dünnen Flüssigkeitsfilms an der inneren Oberfläche eines Rohres durch natürliche Konvektion auftritt. Die Auftriebsströmung wird dabei sowohl durch Temperaturunterschiede als auch durch Konzentrationsunterschiede angetrieben. Ergebnisse für ein Luft/Wasser-System werden gezeigt. Der Einfluß von Rohrlänge und Systemtemperatur auf Impuls-, Wärme- und Stoffübergang wird sehr detailliert untersucht. Der wichtige Einfluß des Flüssigkeitsfilms, der einmal in Richtung des Auftriebs und einmal in Gegenrichtung strömt, wird deutlich gemacht.

ЕСТЕСТВЕННАЯ КОНВЕКЦИЯ В ВЕРТИКАЛЬНОЙ ОТКРЫТОЙ ТРУБЕ, ОБУСЛОВЛЕННАЯ СОВМЕСТНЫМ ВОЗДЕЙСТВИЕМ ТЕПЛОВОЙ И МАССОВОЙ ДИФФУЗИИ

Аннотация—Теоретически исследуется влияние переноса скрытой теплоты при испарении тонкой пленки жидкости на внутренней поверхности трубы на естественную конвекцию, вызванную совместным действием подъемных сил тепловой и массовой диффузии. Представлены результаты для системы воздух–вода при различных режимах. Исследуется влияние длины трубы и температуры системы на перенос импульса, тепла и массы в потоке. Показана важная роль, которую играет пленка жидкости в течении сонаправленных и противоположно направленных потоков, обусловленных подъемными силами.